# Bayesian analysis of stage-fall-discharge rating curves and their uncertainties

Valentin Mansanarez, J. Le Coz, Benjamin Renard, M. Lang, G. Pierrefeu, P. Vauchel

AGU PUBLICATIONS

Water Resources Research

RESEARCH ARTICLE
10.1002/2016WR018916

**Key Points:**
- A Bayesian method with hydraulically interpretable parameters for stage-fall-discharge rating curves
- Sensitivity analyses to available prior information and gaugings
- Application to three twin-gauge stations, with distinct hydraulic configurations

**Correspondence to:**
V. Mansanarez,
valentin.mansanarez@irstea.fr

**Citation:**
Mansanarez, V., J. Le Coz, B. Renard, M. Lang, G. Pierrefeu, and P. Vauchel (2016), Bayesian analysis of stage-fall-discharge rating curves and their uncertainties, *Water Resour. Res.*, *52*, 7424–7443, doi:10.1002/2016WR018916.

Received 15 MAR 2016
Accepted 7 SEP 2016
Accepted article online 24 SEP 2016
Published online 29 SEP 2016



# Bayesian analysis of stage-fall-discharge rating curves and their uncertainties

**V. Mansanarez[1], J. Le Coz[1], B. Renard[1], M. Lang[1], G. Pierrefeu[2], and P. Vauchel[3]**

[1]Irstea, UR HHLY, Hydrology-Hydraulics, Villeurbanne, France, [2]Compagnie Nationale du Rhône, Lyon, France, [3]IRD GET, Toulouse, France

**Abstract** Stage-fall-discharge (SFD) rating curves are traditionally used to compute streamflow records at sites where the energy slope of the flow is variable due to variable backwater effects. We introduce a model with hydraulically interpretable parameters for estimating SFD rating curves and their uncertainties. Conventional power functions for channel and section controls are used. The transition to a backwater-affected channel control is computed based on a continuity condition, solved either analytically or numerically. The practical use of the method is demonstrated with two real twin-gauge stations, the Rhône River at Valence, France, and the Guthusbekken stream at station 0003·0033, Norway. Those stations are typical of a channel control and a section control, respectively, when backwater-unaffected conditions apply. The performance of the method is investigated through sensitivity analysis to prior information on controls and to observations (i.e., available gaugings) for the station of Valence. These analyses suggest that precisely identifying SFD rating curves requires adapted gauging strategy and/or informative priors. The Madeira River, one of the largest tributaries of the Amazon, provides a challenging case typical of large, flat, tropical river networks where bed roughness can also be variable in addition to slope. In this case, the difference in staff gauge reference levels must be estimated as another uncertain parameter of the SFD model. The proposed Bayesian method is a valuable alternative solution to the graphical and empirical techniques still proposed in hydrometry guidance and standards.

## 1. Introduction

Most of the streamflow records are established at water level monitoring stations using stage-discharge functions. Actually, such simple 'rating curves' are valid if the stage-discharge relation is governed by either a section control (upstream of a critical flow section) or a channel control with constant energy slope. Under those assumptions, hydraulics formulas for section controls and for channel controls with wide rectangular cross section can be expressed as simple power functions as follows [*World Meteorological Organization*, 2010; *ISO 1100-2*, 2010]:

$$Q(h)=a(h-b)^c \tag{1}$$

where $Q$ is the discharge, $h$ is the stage, $a$ is a coefficient related to the characteristics of the controlling section or channel, $b$ is an offset, and $c$ is an exponent related to the type of hydraulic control [e.g., *Le Coz et al.*, 2014].

The ideal situation of a channel control is that of a uniform flow when the energy slope is parallel to the water surface slope and to the bed slope. In some cases the energy slope varies over time, generally due to a variable downstream boundary condition (or 'variable backwater'), or sometimes due to transient flow conditions ('varying discharge'). Comprehensive reviews can be found in *Schmidt* [2002] and *Petersen-Øverleir and Reitan* [2009].

The importance of managing hydrometric stations affected by a variable slope has been recognized in hydrometry guidance and standards for long [e.g., *Hall et al.*, 1915; *Réméniéras*, 1949; *Rantz*, 1982; *ISO 9123*, 2001; *World Meteorological Organization*, 2010]. When energy slope is affected by transient flow effects, the resulting stage-discharge hysteresis can be approximated by single-gauge methods [e.g., *Jones*, 1916; *Fenton and Keller*, 2001]. Index velocity systems [e.g., *Le Coz et al.*, 2008; *Nihei and Kimizu*, 2008; *Hoitink et al.*, 2009; *Hidayat et al.*, 2011; *Levesque and Oberg*, 2012] have been developed and increasingly used for streams

affected by variable backwater. However the traditional stage-fall-discharge (SFD) method remains commonly used in such situations. The SFD method requires to measure the fall, hence the water surface slope between the main gauge and an auxiliary gauge usually located further downstream along the same river reach. As long as the flow depth variation along the reach remains limited, the flow is said to be 'gradually varied' and usual friction formulas (Darcy-Weisbach, Manning-Strickler, Chézy) designed for uniform flows can still be applied. According to these friction formulas, discharge is proportional to the square root of the energy slope. Therefore, the real discharge $Q$ can be derived from the fall ratio to a power $N$, close to 1/2, as:

$$Q = Q_r \left(\frac{F}{F_r}\right)^N \tag{2}$$

with $Q_r$ the discharge computed from stage-discharge rating curve established for reference conditions, $F$ the measured fall and $F_r$ the fall established for reference conditions. The reference conditions are the usual flow regime not affected by variable backwater.

Though this method is not fully hydraulically accurate [*Schmidt*, 2002], it proved to be convenient and often produced acceptable discharge estimates at hydrometric stations with variable slope [*ISO 9123*, 2001]. Valuable streamflow records are based on this technique in canals and rivers affected by the water level of lakes, seas, dams or main stems located further downstream [e.g., *Callède et al*., 2001]. Nevertheless, it is still needed to develop practical and rigorous methods for establishing such stage-fall-discharge models and for conducting the uncertainty analysis of the resulting discharge records.

To bring new solutions to this problem, this work builds on the avenue opened by *Petersen-Øverleir and Reitan* [2009]. The Bayesian approach they introduced appears to be a promising way to analyze stage-fall-discharge relations and the related uncertainties. Like other Bayesian methods applied to stage-discharge relations [e.g., *Moyeed and Clarke*, 2005; *Reitan and Petersen-Øverleir*, 2008; *Sikorska et al*., 2013; *Juston et al*., 2014; *Le Coz et al*., 2014] it provides a flexible framework for incorporating prior information on control segmentation and hydraulic extrapolation beyond the largest gauged flows. Some non-Bayesian methods have also been applied to stage-discharge relations [e.g., *Shrestha et al*., 2007; *McMillan et al*., 2010; *Westerberg et al*., 2011; *Morlot et al*., 2014; *Coxon et al*., 2015; *McMillan and Westerberg*, 2015], and might be adapted to the case of SFD relations.

Compared to the original work of *Petersen-Øverleir and Reitan* [2009], we propose a different stage-fall-discharge model. *Petersen-Øverleir and Reitan* [2009] considered the frequent situation when a gauging station is not permanently affected by variable backwater, which requires a two-segment rating curve and a discharge continuity condition:

$$Q(h_1, h_2) = \begin{cases} C_1 (h_1 - h_0)^{b_1} & \text{if } h_2 \le h_0 \quad \text{backwater unaffected} \\ C_1 (h_1 - h_2)^{\eta} (h_1 - h_0)^{b_1 - \eta} & \text{if } h_2 > h_0 \quad \text{backwater affected} \end{cases} \tag{3}$$

where $\eta$ is a parameter and $C_1$ and $b_1$ are hydraulic quantities according to *Petersen-Øverleir and Reitan* [2009] model. Some assumptions of this model are disputable. The first concern is the assumption that the 'cease-to-flow' stage, or offset $h_0$, would be the same for the two controls. A second concern is the statement that the transition to backwater-affected regime occurs when the downstream stage $h_2$ is greater than $h_0$. In this paper, both assumptions will be shown to be disputable from a hydraulic point of view, and models based on different assumptions will be introduced. Moreover, considering the common case of wide and rectangular channel controls, the Manning-Strickler friction formula leads to:

$$Q(h_1, h_2) = \begin{cases} BK_S \sqrt{S_0}\, (h_1 - h_0)^{5/3} & \text{backwater unaffected} \\ BK_S \sqrt{(h_1 - h_2)/L}\, (h_1 - h_0)^{5/3} & \text{backwater affected} \end{cases} \tag{4}$$

where $B$ is the channel width, $K_S$ is the Strickler flow resistance coefficient, $S_0$ is the river bed slope and $L$ the distance between the twin gauges. Matching equations (3) and (4) yields:

$$\begin{cases} C_1 = BK_S \sqrt{S_0} & [\mathrm{m}^{4/3}.\mathrm{s}^{-1}] \text{ and } b_1 = 5/3 & \text{backwater unaffected} \\ C_1 = BK_S L^{-1/2} & [\mathrm{m}^{5/6}.\mathrm{s}^{-1}],\ \eta = 1/2 \text{ and } b_1 = 13/6 & \text{backwater affected} \end{cases} \tag{5}$$

with nonconsistent values of $C_1$ and $b_1$ parameters on the two components of the rating curve model.

In the case where the backwater-unaffected control is no longer a wide rectangular channel but a critical cross section represented as a horizontal crested weir, equation (4) becomes:

$$Q(h_1,h_2)=\begin{cases} CB'\sqrt{2g}\,(h_1-h_0)^{3/2} & \text{backwater unaffected} \\ BK_S\sqrt{(h_1-h_2)/L}\,(h_1-h_0)^{5/3} & \text{backwater affected} \end{cases} \quad (6)$$

where $C$ is the discharge coefficient, $B\prime$ the width of the weir and $g$ the gravity acceleration. Matching equations (3) and (6) yields:

$$\begin{cases} C_1=CB'\sqrt{2g} & [\mathrm{m}^{3/2}.\mathrm{s}^{-1}] \text{ and } b_1=3/2 & \text{backwater unaffected} \\ C_1=BK_SL^{-1/2} & [\mathrm{m}^{5/6}.\mathrm{s}^{-1}],\ \eta=1/2 \text{ and } b_1=13/6 & \text{backwater affected} \end{cases} \quad (7)$$

with again nonconsistent values of $C_1$ and $b_1$ parameters on the two components of the rating curve model.

Probably due to this rating-curve model, the application cases reported by *Petersen-Øverleir and Reitan* [2009] led to unrealistic estimates of some hydraulic exponents and coefficients. Typically, the resulting median values for hydraulic exponents $b_1$ and $b_1 - \eta$ of the two segments (e.g., Table 3: $b_1 = 2.4$ and $b_1 - \eta = 1.99$) were generally found to be inconsistent with the assumed controls, such as a wide, rectangular control channel (1.67) or a horizontal critical section (1.5).

The original contribution of this paper to the Bayesian analysis of stage-fall-discharge rating curves is to introduce a model accounting for gradually varied flows in wide open-channels (section 2). We also establish the segmentation of the rating curve based on continuity constraints between segments governed by a backwater-affected channel control and a backwater-unaffected control, the latter being either a channel control or a section control. The operational applicability is demonstrated using two real situations typical of channel-controlled and section-controlled sites: the Rhône at Valence, France, and the Guthusbekken at station 0003·0033, Norway [*Petersen-Øverleir and Reitan*, 2009], respectively (section 3). The performance of the new method is tested through sensitivity analyses to priors and observations (section 4) using a channel-controlled site that has been comprehensively documented with gaugings (the Rhône at Valence, France). Last, the limitations of stage-fall-discharge rating curves are investigated using a challenging case in a mega-river with variable roughness due to bedforms: the Madeira at Fazenda Vista Alegre, Brazil, affected by the variable backwater of the Amazon River (section 5).

## 2. Methods

### 2.1. Stage-Discharge Controls in Gradually Varied Flows

The variable backwater due to unsteady downstream boundary condition can be caused by the stage fluctuations of a reservoir, a lake, a tidal outlet, or even debris/ice jams or dike break for instance. As in the idealized examples of Figure 1, a station is not always affected by variable backwater, so a transition (assumed to be instantaneous) to at least one unaffected control must be considered. Necessarily, the backwater-affected control is a channel control since a section control does not depend on the energy slope, nor on the flow conditions downstream of the critical cross-section. Assuming that both the main and auxiliary gauges are located within a gradually varied flow, we apply the conventional Manning-Strickler friction formula, assumed to be valid for this kind of slightly nonuniform flows. When the flow is rapidly varied or heavily impounded, like in a lake or a reservoir, friction formulas like the Manning-Strickler equation do not apply any longer.

The backwater-unaffected control can be either a section control (flow choked upstream of a critical section) or a channel control (friction dominated flow). We will introduce two different SFD models for the section control (SFD-s) and the channel control (SFD-c) situations. Considering two controls may not be enough, especially at stations where an unaffected channel control or a variable slope channel control can both take over a low-flow section control. Obviously, other perturbations of the controls may not be captured by measuring the variable slope, especially variable roughness (due to weeds, ice cover, bedforms, etc.), additional head losses in compound channel flows and rating shifts due to morphodynamical evolution of the channel [e.g., *Westerberg et al.*, 2011; *Morlot et al.*, 2014]. Only the issue of variable roughness will be addressed in this paper, as an example of the limitations of stage-fall-discharge rating curves (see section 5).

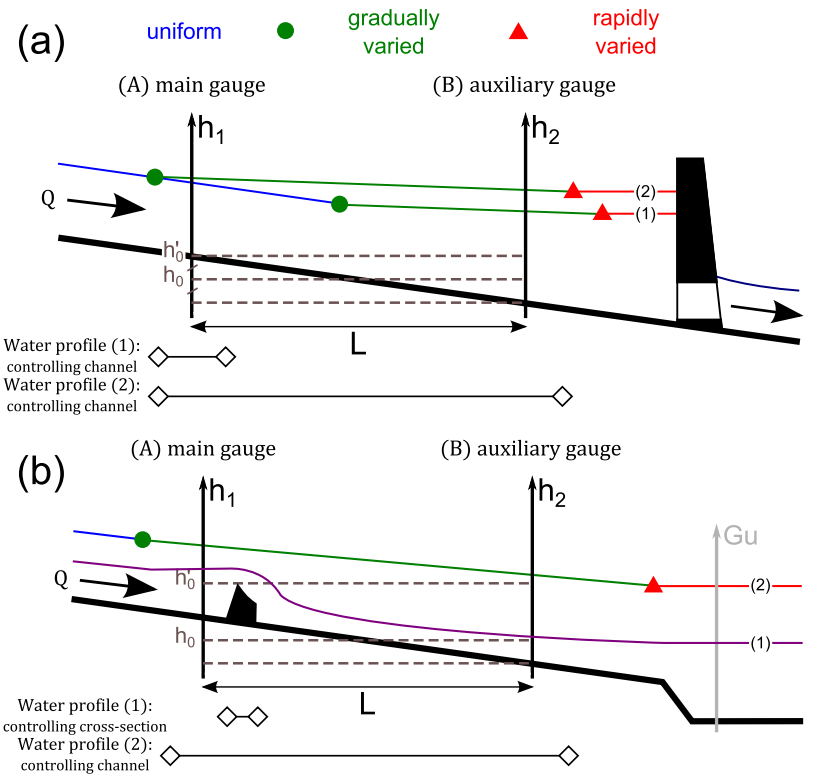


**Figure 1.** Typical transitions for stage-fall-discharge model: (a) from nonaffected channel control (water profile (1)) to a variable slope channel control (water profile (2)) upstream of a dam; (b) from nonaffected section control (water profile (1)) to variable slope channel control (water profile (2)) upstream of a rivers' confluence or a lake. For the Guthusbekken case, the downstream station $h_2$ is located in the lake (Gu). Red triangles correspond to the transition between gradually varied flow and rapidly varied flow whereas green circle to the transition between uniform flow and gradually varied flow.

Figure 1a shows a typical channel control situation upstream of a dam but would equivalently apply to any type of variable downstream boundary condition. Depending on upstream (discharge) and downstream (stage) boundary conditions, the primary gauge may be located within a fairly uniform flow (cf. water profile (1)) or within a gradually varied flow (cf. water profile (2)). It is very important to realize that the two controlling channels are not the same, the former being centred around the primary gauge, whereas the latter is mainly located in between the two gauges. A critical implication is that offsets $h'_0$ (mean bottom level at the main gauge) and $h_0$ (mean bottom level between both gauges) cannot be considered to be the same, as assumed by *Petersen-Øverleir and Reitan* [2009]. Moreover, it clearly appears that their transition condition when the auxiliary stage $h_2$ is equal to $h_0$ does not apply since $h_2$ is likely to always remain greater than $h_0$ in such a deep, flat channel configuration. When velocity head is negligible ($V^2/2g \ll h$), the friction slope can be approximated by the water surface slope, estimated by $(h_1-h_2)/L$ considering that the distance $L$ is short enough to have a linear water profile between the twin gauges (gradually varied flow assumption).

Figure 1b shows a typical section control that may be drowned or not, according to discharge and water level at a lake located downstream (again, any type of variable downstream boundary condition may apply). The submersion of the weir does not necessarily imply a nonunique rating curve: the channel control that takes over may be affected or not by variable backwater from the lake. Again, the assumption that both section control (cf. water profile (1)) and channel control (cf. water profile (2)) have equal offsets $h_0$ (offset of the channel control) and $h\prime_0$ (weir crest elevation) appears to be inadequate. Moreover, such a transition is usually predicted to occur when the stage downstream of the weir $h_{ds}$ exceeds the weir crest elevation $h_0$ (as used by *Petersen-Øverleir and Reitan* [2009]) or when $(h_{ds}-h_0) < \lambda(h_1-h_0)$ with $\lambda \approx 2/3$. Actually such weir submergence conditions cannot be applied since usually the auxiliary gauge is not located in the flow re-establishment section downstream of the control, rather much further downstream. As a consequence, measured $h_2$ is substantially lower than $h_{ds}$ and the relation between both stages is not straightforward since it depends on the hydraulic conditions along the long reach between the weir and the auxiliary gauge.

### 2.2. Stage-Fall-Discharge Rating Curve Models

#### 2.2.1. SFD-c Model: Channel Controls With Constant and Variable Slope

A channel control is modeled using a three-parameter power-law, after simplification of the Manning-Strickler equation for a wide, rectangular cross section: wetted area $A \approx B(h_1 - h_0)$ and hydraulic radius $R_h \approx h_1 - h_0$, with $B$ the mean channel width and $h_0$ the average bottom level at primary gauge. The backwater-unaffected control is assumed to have a constant friction slope $S_0$, whereas the variable slope of the backwater-affected control is approximated by $(h_1 - h_2)/L$ where $L$ is the longitudinal distance between the two gauges.

Therefore, equation (4) can be rewritten as follow:

$$Q(h_1, h_2) = \begin{cases} K_S B (h_1 - h_0)^M \sqrt{(h_1 - h_2 - \delta_h)/L} & \text{if} \quad h_1 < \kappa(h_2) \quad \text{(variable slope)} \\ K'_S B' (h_1 - h'_0)^M \sqrt{S_0} & \text{if} \quad h_1 \geq \kappa(h_2) \quad \text{(channel control)} \end{cases} \tag{8}$$

where $\delta_h$ is the difference in datum reference levels between the auxiliary gauge and the main gauge, and $M$ an exponent related to the assumed friction equation and the cross-sectional shape. $M$ is equal to 5/3 for Manning-Strickler equation in a wide rectangular channel. Unlike existing stage-fall-discharge approaches, we deem it important to estimate the parameter $\delta_h$ as it may be affected by significant uncertainties. Parameter $\delta_h$ is independent of parameters $h_0$ and $h\prime_0$: the former is the measurement errors in the levelling of the datum of the staff gauges whereas the latter are due to the limited knowledge of the river geometry, with respect to the staff gauge references (no absolute levelling included).

Compared with *Petersen-Øverleir and Reitan* [2009] we use two separate $h_0$ and $h'_0$ parameters for the two channel controls to avoid hydraulic conflicts. Moreover we assume the flow resistance coefficients $K_S$ and $K'_S$ and the widths $B$ and $B\prime$ are different. In many cases, the controlling channels are similar for both backwater-affected and backwater-unaffected conditions. In such cases, equation (8) can be rewritten with $K'_S = K_S$ and $B' = B$.

Another important difference with the SFD model proposed by *Petersen-Øverleir and Reitan* [2009] is that the transition condition comes as a discharge continuity condition for $h_1 = \kappa(h_2)$ in equation (8), which leads to:

$$K_S B (\kappa(h_2) - h_0)^M \sqrt{(\kappa(h_2) - h_2 - \delta_h)/L} - K'_S B' (\kappa(h_2) - h'_0)^{M'} \sqrt{S_0} = 0 \tag{9}$$

The Newton-Raphson algorithm is used to solve equation (9) and find the transition stage $\kappa(h_2)$.

#### 2.2.2 SFD-s Model: A Section Control and a Variable Slope Channel Control

If the backwater-unaffected control is a section control, it can be modeled as an equivalent weir. Therefore, considering the most common situation, i.e., a natural or artificial control that can be approximated as a horizontal-crested weir, equation (6) can be rewritten as:

$$Q(h_1, h_2) = \begin{cases} C B' \sqrt{2g} (h_1 - h'_0)^{M'} & \text{if} \quad h_2 < \kappa'(h_1) \quad \text{(section control)} \\ K_S B (h_1 - h_0)^M \sqrt{(h_1 - h_2 - \delta_h)/L} & \text{if} \quad h_2 \geq \kappa'(h_1) \quad \text{(variable slope)} \end{cases} \tag{10}$$

where the width $B'$ of the weir often differs from the channel width $B$, the discharge coefficient $C$ is approximatively equal to 0.4, the exponent $M'$ is close to 3/2 and the gravity acceleration $g$ is given equal to 9.81 m.s$^{-2}$.

Following *Petersen-Øverleir and Reitan* [2009], we do not consider the possible occurrence of a third control, i.e., a constant-slope channel control, and we assume therefore that variable backwater occurs as soon as the section control is submerged. Again, the transition between the backwater affected and unaffected controls is computed through a discharge continuity condition for $h_2 = \kappa'(h_1)$, which can now be solved explicitly:

$$\kappa'(h_1) = h_1 - \delta_h - L \left( \frac{C B' \sqrt{2g}}{K_S B} \right)^2 \frac{(h_1 - h'_0)^{2M'}}{(h_1 - h_0)^{2M}} \tag{11}$$

Unlike the case of channel controls, the transition condition is governed by the stage at the auxiliary gauge: the weir is submerged and backwater affected channel control takes over when stage $h_2$ exceeds $\kappa'(h_1)$.

### 2.3. Inference/Parameter Estimation

The proposed method is an extension of the Bayesian framework associated with the BaRatin method [*Le Coz et al.*, 2014]. The main updates and extensions made for this study are described hereafter. The reader is referred to *Le Coz et al.* [2014] for a comprehensive description of the existing BaRatin framework and an overview of its principles.

Gaugings $(\tilde{h}_{1,i}, \tilde{h}_{2,i}, \tilde{Q}_i)_{i=1,N}$ are seen as estimates of the real values $(h_{1,i}, h_{2,i}, Q_i)_{i=1,N}$ of stages and associated discharges. We further assume that stage errors are negligible compared to discharge errors:

$$\begin{cases} \tilde{h}_{1,i} = h_{1,i} \\ \tilde{h}_{2,i} = h_{2,i} \\ \tilde{Q}_i = Q_i + \epsilon_{Q_i} \qquad \text{with} \qquad \epsilon_{Q_i} \overset{\text{indep.}}{\sim} \mathcal{N}(0, u_{Q_i}) \end{cases} \tag{12}$$

where the standard deviations $u_{Q_i}$ are assumed to be known and the discharge errors are assumed independent. Depending on their measurement technique and field procedure, uncertainty values were assigned to gaugings based on the typical results of available propagation methods [e.g., *Despax et al.*, 2016] and in-situ intercomparisons [e.g., *Le Coz et al.*, 2016].

The stage-discharge relationship is given by:

where are the rating curve parameters, are the structural errors and are the standard deviations of the structural errors .

As discussed by *Le Coz et al.* [2014], an affine function for modelling the standard deviation is used. This affine model assumes that this standard deviation is dominated at low flows by a constant term $\gamma_1$ whereas at high flows the error is proportional to the discharge estimation . Wide uniform distributions (between 0 and $10^6$) are used as priors for both $\gamma_1$ and $\gamma_2$ parameters: these parameters are let to be inferred from the gaugings. We also assume that the structural errors are independent. This assumption may be acceptable when the gaugings are separated by a duration of several weeks or months. However, it is more problematic in terms of uncertainty propagation, because independent structural errors will be generated to produce uncertain hydrographs, even for consecutive time steps separated by a few minutes or hours. This is a difficult issue that has no complete solution as far as we know, and we refer the reader to the in-depth discussion in *Le Coz et al.* [2014] for more details on this topic.

Combining equations (12) and (13) yields the following stage-fall-discharge relation between observed values, assuming independence between and :

Unknown quantities that have to be estimated are the parameters of the rating curve and the parameters of the structural error model. Equation (14) allows computing the likelihood function as described in *Le Coz et al.* [2014]. Combined with prior distributions for and , this yields a posterior distribution that can be explored by MCMC sampling [*Renard et al.*, 2006]. In the following sections, uncertainty bounds are computed from the MCMC samples with a probability level of 95% (i.e., 2.5% and 97.5% percentiles), as usually done in hydrometric applications [*ISO/TS 25377*, 2007]. The maximum *a posteriori* (MAP) estimator is used to estimate the rating curve. This estimator is the mode of the posterior density.

## 3. Application to Typical Cases With Channel and Section Controls

### 3.1. Channel-Control Case: The Rhône River at Valence

The Rhône River has a mean interannual discharge of at its outlet (Beaucaire station, catchment area of ). It flows along 812 km from a glacier in Switzerland, through Lake Geneva down to the Mediterranean Sea.

At Valence station the Rhône drains a catchment area of (68% of the whole catchment area). The primary gauge is located just upstream of a motorway bridge (Longitudinal position: Kilometric Point 109.7 km, GPS locations: E, N). The streamwise distance $L$ between the two stations is known to be . The friction slope $S_0$ at the highest flows is not accurately measured but is estimated to be roughly .

Figure 2 shows different cross-sectional profiles all along the section between the twin gauges. Over approximately 2 km (down to the Kilometric Point 111.5 km) downstream of the primary gauge, the channel is fairly uniform and rectangular with a mean width ; then the channel gradually expands on its left side up to the auxiliary

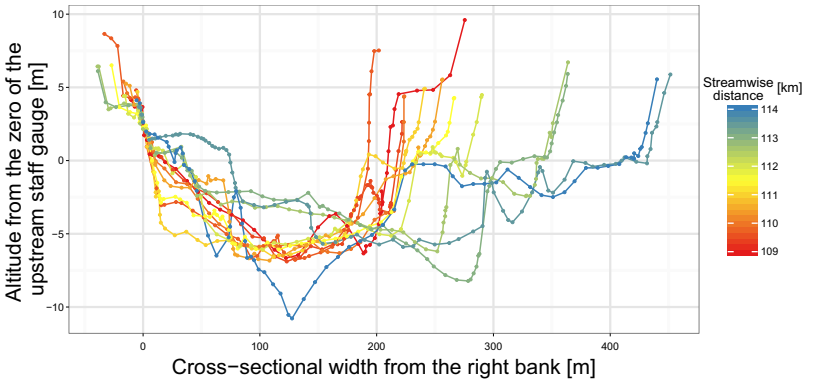


**Figure 2.** The Rhône River at Valence: cross-sectional profiles between the main and auxiliary stations.

station (Longitudinal position: Kilometric Point , GPS locations: E, N). The mean width between the two gauges differs from that around the primary gauge and is set to . Both channel control offsets, $h_0$ and , are set to . From existing hydraulic models, both Strickler flow resistance coefficients $K_S$ and  are set to . The datum difference $\delta_h$ between the two staff gauges is accurately leveled by the Compagnie Nationale du Rhône (CNR) and is set to 0 m . Corresponding priors are summarized in Table 1.

68 gaugings were performed at the Valence station. These gaugings are densely distributed from  to , which roughly corresponds to the 50 year flood. The mean annual discharge is . Figure 3 shows the estimated rating curves as  plots with the 95% total uncertainty envelopes. The SFD rating curves are plotted for 5 $h_2$ values which correspond to 4 available gaugings (, 1.93, 2.40 and ) and to the maximum $h_2$ value () recorded over the last 40 years. As expected from the hydraulic analysis, individual rating curves for distinct $h_2$ values merge with the unaffected channel control curve when $h_1$ exceeds the transition threshold .

For the sake of comparison, results from the standard stage-discharge (SD) model is also computed with a single constant-slope channel control, using the same prior information as for the SFD model. The SD model is clearly not adequate for capturing the variable backwater effect. Despite the MAP rating curve of this model agreeing with the highest gaugings (i.e., the unaffected channel control), it obviously fails to describe the scattered low-flow gaugings (cf. Figure 3). The associated total uncertainties are extremely high at both low and high flows. On the opposite, all the MAP rating curves estimated by the SFD model agree with gaugings and have much smaller uncertainties: total uncertainty is lower than  for discharges above  (cf. Figure 4). Relative errors of MAP predictions compared to observations are also small and decrease with discharge. The lower agreement at very low flows may be explained by the lack of low-flow gaugings available for calibrating the model (only 3 gaugings at ).

The SD and SFD rating curves can be used to propagate stage time series into discharge time series (in this paper we always estimate instantaneous discharges, at the highest possible temporal resolution). Only rating curve errors are taken into account in such a propagation (i.e., stage errors are ignored). Figure 5 illustrates the resulting

**Table 1.** Parameters, Prior Distributions and Results of the Bayesian Analysis of the Stage-Fall-Discharge Rating Curve of the Rhône River at Valence

| BaRatin Parameter | Physical Parameter | Units | Prior Distribution[a] | SFD-c Results: MAP $[Q_{2.5}; Q_{97.5}]$ |
|---|---|---|---|---|
| $\theta_1$ | $K_{SB}$ | $m^{\frac{4}{3}}.s^{-1}$ | $\mathcal{N}(6000, 1582)$ | 6712 [5641; 8578] |
| $\theta_2$ | $h_0$ | m | $\mathcal{N}(-3, 1)$ | −4.51 [−5.29; −3.69] |
| $\theta_3$ | $M \simeq 5/3$ | | $\mathcal{N}(1.6667, 0.025)$ | 1.67 [1.62; 1.71] |
| $\theta_4$ | $L$ | m | $\mathcal{N}(3900, 100)$ | 3898 [3697; 4091] |
| $\theta_5$ | $h'_0$ | m | $\mathcal{N}(-3, 1)$ | −1.43 [−2.16; −1.15] |
| $\theta_6$ | $K'_S B' \sqrt{S_0}$ | $m^{\frac{4}{3}}.s^{-1}$ | $\mathcal{N}(171, 46)$ | 269 [216; 304] |
| $\theta_7$ | $\delta_h$ | m | $\mathcal{N}(0, 0.025)$ | −0.025 [−0.035; −0.018] |
| $\theta_8$ | $M' \simeq 5/3$ | | $\mathcal{N}(1.6667, 0.025)$ | 1.68 [1.64; 1.73] |
| $\gamma_1$ | | $m^3.s^{-1}$ | $\mathcal{U}(0, 10^6)$ | 69 [45; 91] |
| $\gamma_2$ | | | $\mathcal{U}(0, 10^6)$ | 0.0009 [0.0002; 0.022] |

[a]The symbol $\mathcal{N}(\mu, \sigma)$ corresponds to the normal distribution with mean $\mu$ and standard deviation $\sigma$. The symbol $\mathcal{U}(a, b)$ corresponds to the uniform distribution on the interval $[a, b]$.

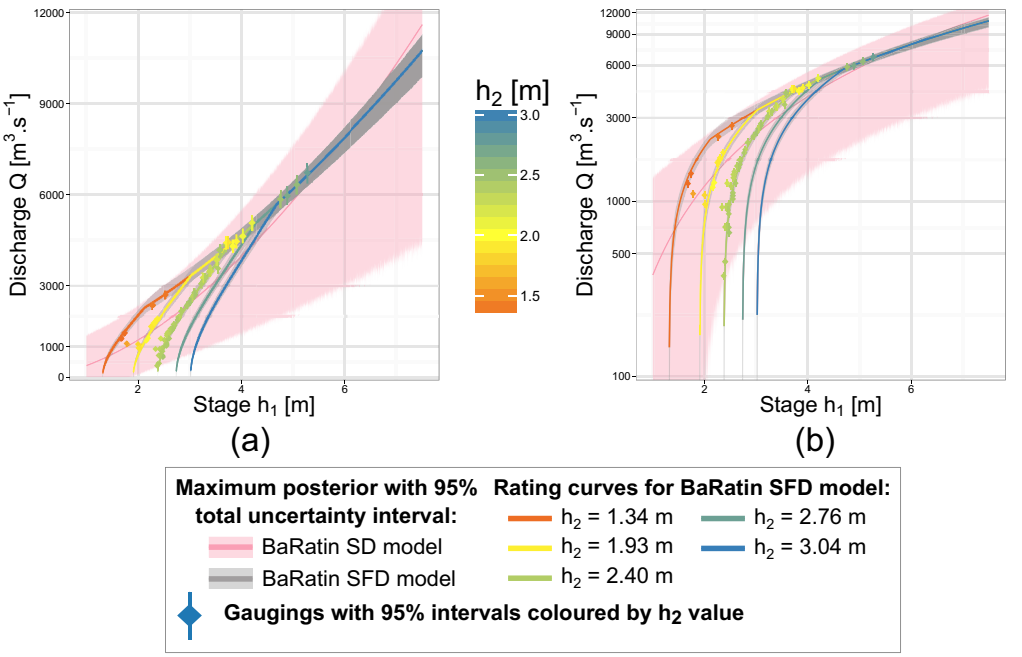


**Figure 3.** The Rhône River at Valence: stage-discharge representation of the stage-fall-discharge (SFD) and stage-discharge (SD) models, with discharges in (a) natural scale and (b) logarithm scale. The SFD rating curves are plotted for 5 values of $h_2$ corresponding to available gaugings ($h_2$ = 1.34, 1.93, 2.40 and 2.76 m) and to the maximum recorded value (3.04 m) over the last 40 years.

uncertain hydrographs for the September-November 1993 period, which covers the highest flood ever measured at the Valence station. Again, total uncertainties computed by a standard stage-discharge rating curve (SD model) are extremely large: more than for low flows and between and for high flows. Moreover the SD model seems to underestimate high flows. This assessment is clear on the first and fourth gaugings on Figure 5. When the discharge is higher than the discharge associated with stage transition, both SFD and SD model have the same formulation (channel control part in equation (8)) but their parameters differ ( and ) because there are no longer estimated on only high flows but also on low flows for the SD model. The BaRatin SFD model shows much better performance. High flow measurements are accurately estimated by the MAP rating curve and the related uncertainties do not exceed for discharges above . The model clearly makes the transition from

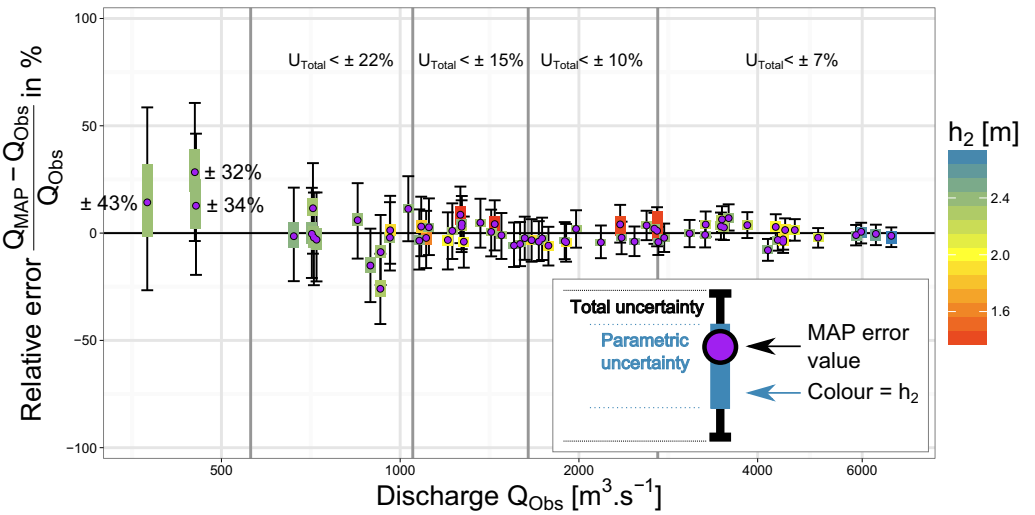


**Figure 4.** Application of the stage-fall-discharge (SFD) model to the Rhône River at Valence: relative errors between the maximum *a posteriori* discharges ($Q_{MAP}$) and the gaugings ($Q_{Obs}$). Error bars represent the parametric and total 95% uncertainty bounds of the discharge estimates, with $h_2$ values colour-coded.

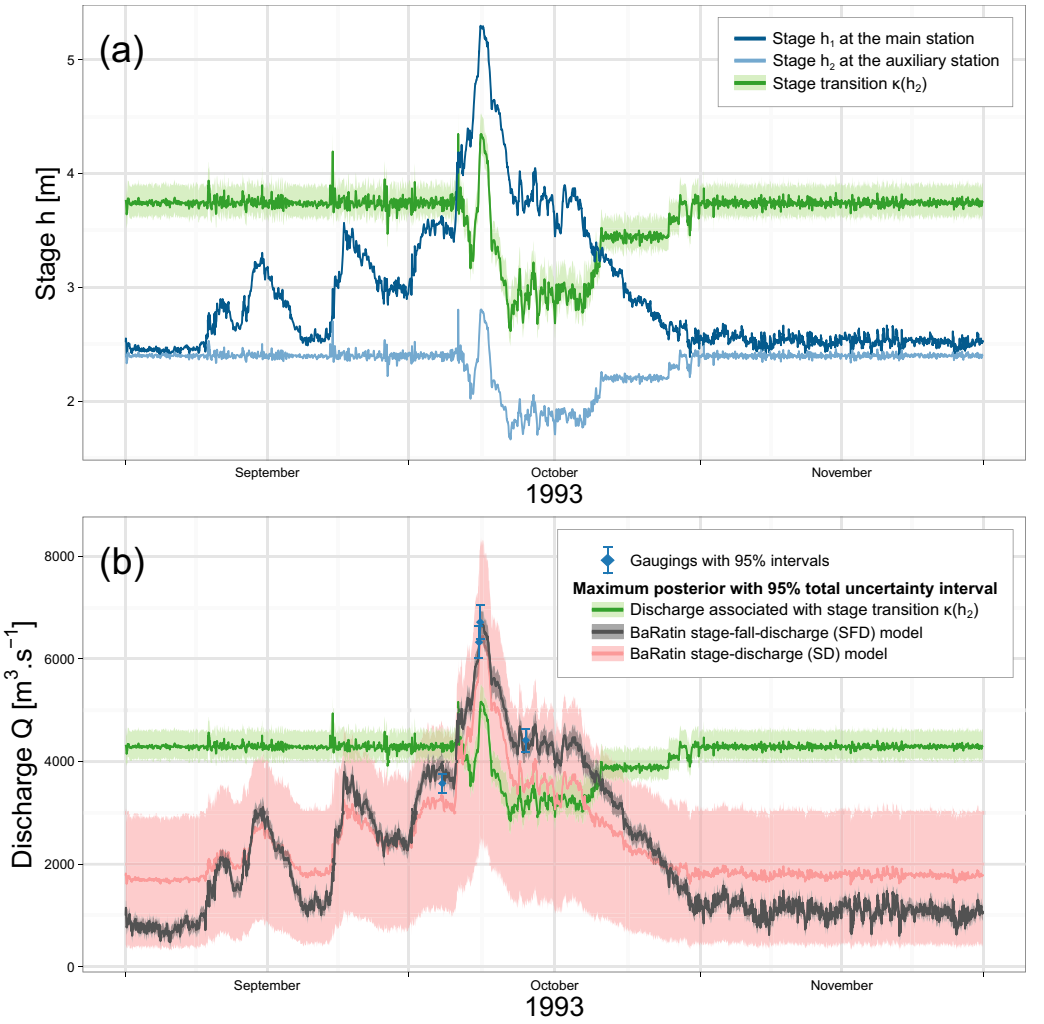


**Figure 5.** The Rhône River at Valence, flood of October 1993: (a) stage records $h_1$ and $h_2$ at respectively the main and auxiliary stations with the estimated stage transition $\kappa(h_2)$ of the stage-fall-discharge (SFD) model; (b) instantaneous discharge estimated by the SFD and stage-discharge (SD) models.

backwater affected to backwater unaffected channel control, when discharge $Q$ exceeds the discharge threshold for . That discharge threshold, plotted in green with its uncertainties in Figure 5, is found to decrease during the flood due to a concurrent decrease in $h_2$.

### 3.2. Section-Control Case: Guthusbekken at Station 00030033

For an application of the proposed SFD-s model, we use the study of the Guthusbekken stream at station 00030033 in Norway fully described in *Petersen-Øverleir and Reitan* [2009] who shared the data. It is a small, 2 m wide stream contracted to  as the flow goes through a canyon and a natural sill of  fall before widening up to  as it enters into the lake Vansjø. The critical section is periodically drowned due to variable backwater effects from the lake when level gets high. The main gauge is located  upstream of the sill whereas the auxiliary gauge is actually located in the lake itself (cf. Figure 1b, mark Gu), at a distance of about  from the main gauge. This situation is not ideal, since the measured fall divided by the constant distance between gauges may then be not representative of the actual water slope in the gradually varied flow section.

27 gaugings were performed at the Guthusbekken station and 8 among them are reported to be the only ones affected by variable backwater. Those 8 measurements are actually four ADCP transects repeated twice, and 14 out of the backwater-unaffected 19 gaugings are also replicates. As a consequence, only 16 independent gaugings could be derived from the whole data set. Despite the limitations of this case study,

**Table 2.** Parameters, Prior Distributions and Results of the Bayesian Analysis of the Stage-Fall-Discharge Rating Curve of Guthusbekken

| BaRatin Parameter | Physical Parameter | Units | Prior Distribution | SFD-s Results: MAP $[Q_{2.5}; Q_{97.5}]$ |
|---|---|---|---|---|
| $\theta_1$ | $K_S B$ | $m^{\frac{4}{3}}.s^{-1}$ | $\mathcal{N}(80, 28.3)$ | 44.0 [34.2; 51.3] |
| $\theta_2$ | $h_0$ | m | $\mathcal{N}(25.32, 2)$ | 25.12 [25.02; 25.18] |
| $\theta_2$ | $M = 5/3$ | | $\mathcal{N}(1.6667, 0.025)$ | 1.672 [1.615; 1.715] |
| $\theta_4$ | $L$ | m | $\mathcal{N}(1400, 50)$ | 1417 [1304; 1498] |
| $\theta_5$ | $h'_0$ | m | $\mathcal{N}(25.32, 0.01)$ | 25.331 [25.324; 25.337] |
| $\theta_6$ | $CB'\sqrt{2g}$ | $m^{\frac{3}{2}}.s^{-1}$ | $\mathcal{N}(2.7, 0.3)$ | 1.12 [1.05; 1.19] |
| $\theta_7$ | $\delta_h$ | m | $\mathcal{N}(0, 0.1)$ | 0.0138 [0.0061; 0.0191] |
| $\theta_8$ | $M' = 3/2$ | | $\mathcal{N}(1.5, 0.025)$ | 1.507 [1.465; 1.552] |
| $\gamma_1$ | | $m^3.s^{-1}$ | $\mathcal{U}(0, 10^6)$ | $9.3\times10^{-4}$ $[2.0\times10^{-4}; 4.5\times10^{-3}]$ |
| $\gamma_2$ | | | $\mathcal{U}(0, 10^6)$ | 0.031 [0.0029; 0.078] |

it is the best documented at hand, and equation (10) was applied to model the unaffected section control and the variable slope channel control.

From the description of the stream bed within a canyon, the Strickler flow resistance coefficient $K_S$ of the stream is guessed to be equal to . As described above, the mean width $B$ between the two gauges is set to and the width of the sill is set to . The distance between the two gauges is set to . Ignoring the contraction effects, the sill can be approximated by a horizontal weir with discharge coefficient . The crest elevation, , is precisely assessed as whereas the channel offset, $h_0$, is left imprecise around . The datum difference $\delta_h$ is set up to . Both exponents $M$ and related to the nature and shape of the controls (wide rectangular channel and horizontal weir) are precisely specified respectively to and , based on hydraulic formulas. These priors are summarized in Table 2. The BaRatin stage-discharge (SD) model with a single section control is also applied, using the same prior information as for the SFD model.

Figure 6 shows the results of the application of the BaRatin SFD-s model for section controls, as representations with the 95% total uncertainty intervals. The SFD rating curves are plotted for 5 $h_2$-values corresponding to one section control gauging () and to four gaugings affected by variable backwater (, 25.64, 25.72 and ). The stage-discharge rating curve computed for the backwater-unaffected section control is plotted as a black dotted line. MAP values and 95% credibility intervals of each parameter of the SFD-s model are summarized in Table 2. Gaugings corresponding to the unaffected section control are well seen on those representations (cf. Figure 6) as they follow the weir law curve irrespective of the $h_2$-values. Gaugings affected by variable backwater are also well identified by the model, in accordance with statements by *Petersen-Øverleir and Reitan* [2009] on the hydraulic situation of these gaugings.

Figure 7 shows the agreement between predicted and gauged discharges as relative errors. MAP rating curves estimated by the SFD-s model agree well with gaugings: error values are low. Total uncertainty envelopes are acceptable (less than at high flows) and have the same width at high flows irrespective of the $h_2$ value. Uncertainty envelopes are large at low flow (up to for the total uncertainty).

The relative contribution of the parametric uncertainty to the total uncertainty decreases when discharge decreases (cf. figure 7). Parameter of the weir equation takes posterior values more than twice smaller than prior values (cf. Table 2). Prior information on this parameter appears to be in disagreement with the information found in the gaugings: a single horizontal weir may not represent well the complexity of this natural control. This cannot be explained without further investigation of the site conditions, especially the geometry of the canyon and its contracted section, and the possible transition to backwater-unaffected channel control for highest stages.

To sum up, the BaRatin SFD-s model for section control produces acceptable discharge estimates for the Guthusbekken station: the agreement of predicted (MAP) versus gauged discharges is good (less than for ). However those results yield hydraulically questionable rating curves. The hydraulic configuration of this station may be more complex than assumed: channel within a complex canyon, auxiliary gauge located in the lake, transition to backwater-affected control possibly not well defined, and transition to channel control at high flow possibly overlooked. The scarcity of independent measurements, especially for backwater-affected situations, also challenges the application of the model to that case. Consequently, additional investigations in the directions described above may lead to a more adequate SFD model, which may help in further reducing uncertainty.

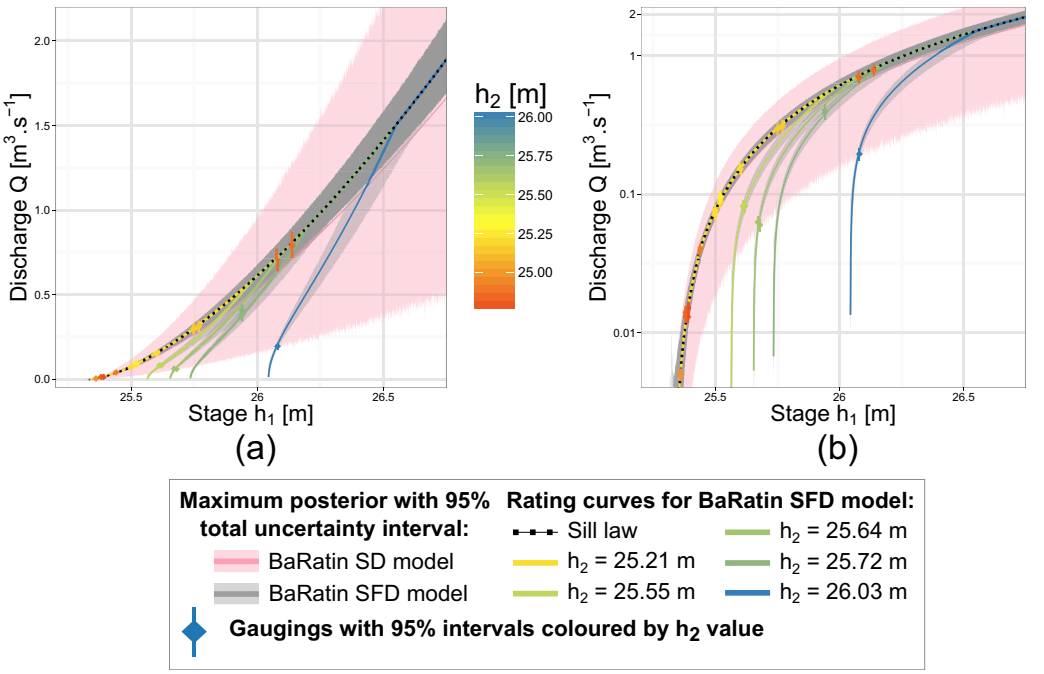


**Figure 6.** The Guthusbekken stream at station 0003 · 0033, Norway: stage-discharge representation of the stage-fall-discharge (SFD) and stage-discharge (SD) models, with discharges in (a) natural scale and (b) logarithm scale. The SFD rating curves are plotted for 5 $h_2$-values corresponding to available gaugings (25.21, 25.55, 25.64, 25.72 and 26.03 m). The sill law computed by the SFD model is added in dark dotted line.

## 4. Sensitivity to Available Information

The SFD-c model (cf. equation (8)) is used to perform sensitivity analyses on the Rhône River at the Valence station.

### 4.1. Sensitivity to Prior Information

Several sets of priors are used to determine which parameters require informative priors and which ones are easily inferred from the data. The first set of priors includes all the available prior information (see prior distributions in Table 1). This set is named "fully informative priors." In the other eight sets of priors, named

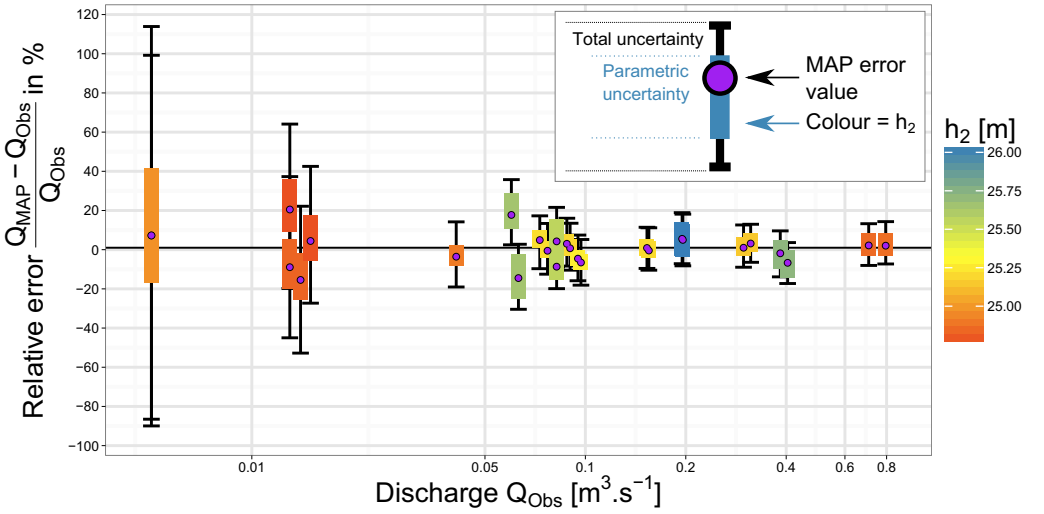


**Figure 7.** Application of the stage-fall-discharge (SFD) model to the Guthusbekken stream at station 0003 · 0033 in Norway: relative errors in percentage between the maximum *a posteriori* discharges ($Q_{MAP}$) and the discharge observations ($Q_{Obs}$). Error bars represent the parametric and total 95% uncertainty bounds of the discharge estimates, with $h_2$ values colour-coded.

"noninformative priors," the precise prior distribution of one of the 8 parameters has been replaced by a wide uniform, noninformative distribution.

Results from this prior sensitivity analysis are shown in Figure 8, which represents for each parameter the prior density (in black), the posterior density associated with the fully informative prior (in pink) and posterior densities associated with the 8 noninformative prior sets.

The longitudinal distance *L* requires prior information to be identified, otherwise its posterior density is very vague and encompasses physically unrealistic values. When the prior of this parameter is more precise, its posterior density matches with prior density. This illustrates that this parameter cannot be inferred from the gauging data only and instead requires prior information. Similarly, parameters *M* and  also require precise informative priors.

Offsets $h_0$ and  can easily be inferred from the information contained in the gaugings: posterior densities are more precise than prior densities. Informative priors on those parameters are not absolutely necessary. However, they can reduce correlation effects with other parameters. Indeed parameters  and  appear to be correlated and any lack of prior information on one of them can propagate to the two other ones (Figure 8, last row). Figure 8 shows that if a noninformative prior on  is assumed, the posterior density of  keeps close to the prior distribution and the posterior density of offset  differs from other prior sets.

The datum difference $\delta_h$ can be inferred from the data and seems to have no direct connection with other parameters. The  product can be identified from the data as well. However, strong correlations between parameters , $h_0$ and *M* impose to have precise prior information on at least two of them.

### 4.2. Sensitivity to Observations (Gaugings Data Set)

An important issue for the management of stations affected by backwater influence is to establish a gauging strategy in order to optimize rating curve estimations and uncertainty assessment. In this section the sensitivity of the stage-fall-discharge model to the gauging data set is investigated still using the Valence case. Several gauging subsamples are used: (1) gaugings covering the whole range, (2) high-flow gaugings only, (3) low-flow gaugings only, (4) gaugings with , (5) gaugings with . For each of the 5 subsamples only 16 gaugings are used to calibrate the stage-fall-discharge model and cross-validation is performed on other gaugings.

The results of this analysis are summarized in Figure 9. As expected, using only high-flow gaugings (2) for calibrating the model yields larger uncertainties on low flows, and brings MAP errors as large as . It may even happen that very low discharges cannot be estimated: the MAP value of the $h_0$ parameter may indeed be higher than the $h_1$ value of the lowest gaugings. This is because the  and $h_0$ parameters of the SFD model for low flows (cf. variable slope part in equation (8)) have uncertain priors and are poorly identified from the data.

On the other hand, using only low-flow gaugings (3) reduces parametric uncertainties at low flows but the model does not precisely identify high flow parameters from the data. Results for  and  remain close to their wide priors. High flow estimates are therefore affected by large uncertainties.

Using only gaugings with low values of $h_2$ (subsample (4)) seems to be an acceptable strategy. Similar to the whole panel (1), MAP error values are centred around zero and the uncertainties are small. Nevertheless, this strategy holds only if all the discharge range is represented. In fact, it may even be problematic at very low flows: for this order of discharge, $h_2$ values are always quite high. In Figure 9 (4), parametric uncertainties on low discharges are larger than those for the whole range.

Finally, using gaugings with a nearly constant $h_2$ value (, subsample (5)) leads to increased uncertainties of discharge estimates compared with the 'whole range', even if all the discharge range is sampled: parametric uncertainties are higher, which shows the difficulty of the model to estimate 'backwater' parameters when the covariate $h_2$ is not variable enough.

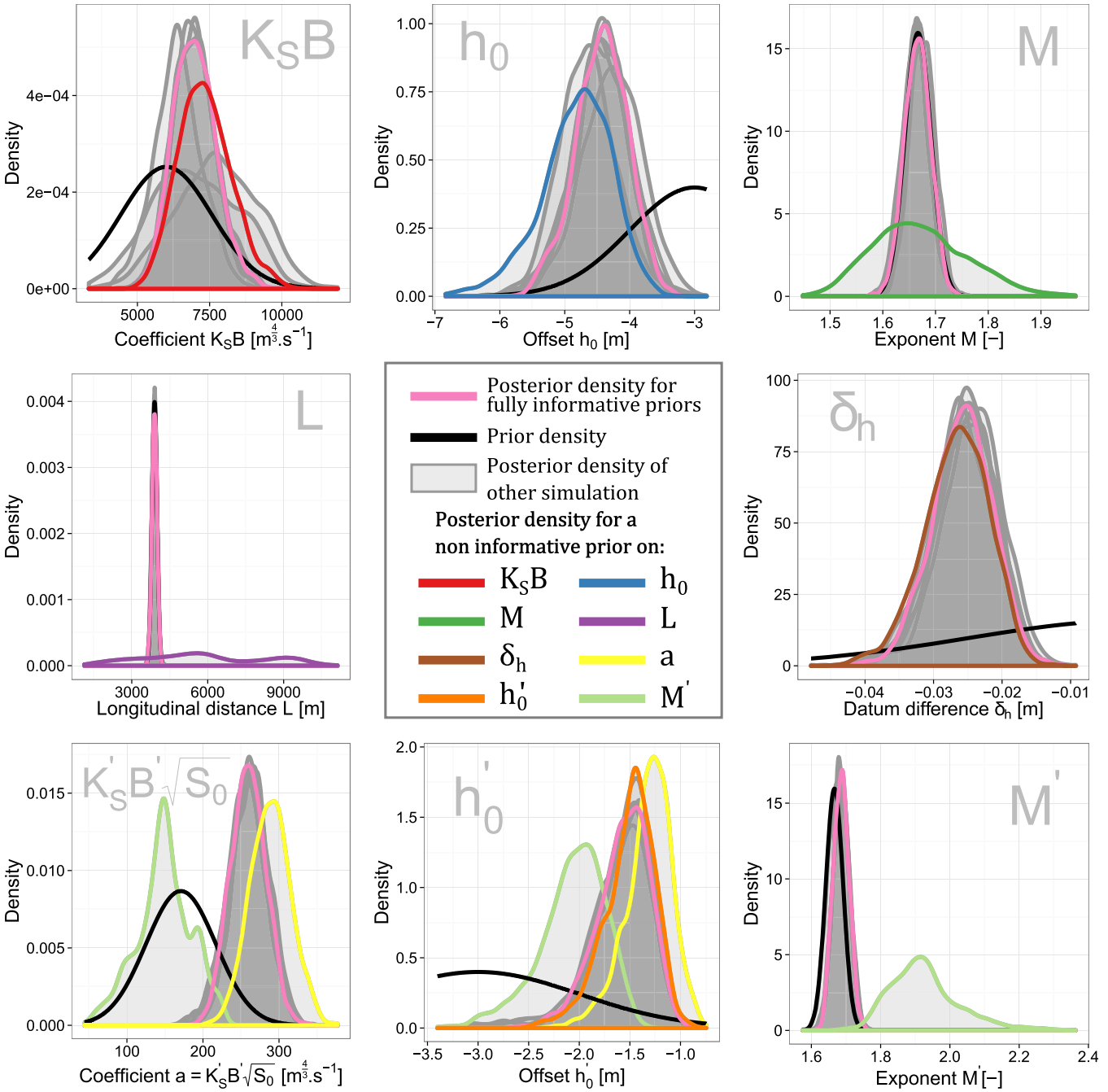


**Figure 8.** Prior sensitivity analysis applied to the Rhône River at Valence: posterior and prior densities of rating curve parameters for fully or partially informative priors.

## 5. Application to a Challenging Case

### 5.1. The Madeira River at Fazenda Vista Alegre

The Madeira River is one of the two largest tributaries of the Amazon (including the Solimoes) by mean discharge, the other one being the Rio Negro. Arguably, the Madeira River would rank between the 4th and 8th largest rivers by mean discharge in the world [e.g., *Latrubesse*, 2008].

The main hydrometric station is at Fazenda Vista Alegre (GPS locations: S, W), Brazil, approximatively upstream of the auxiliary station of Borba (GPS locations: S, W). The Fazenda station covers a basin area of with a mean interannual discharge of . It is located at the downstream part of the catchment and is strongly

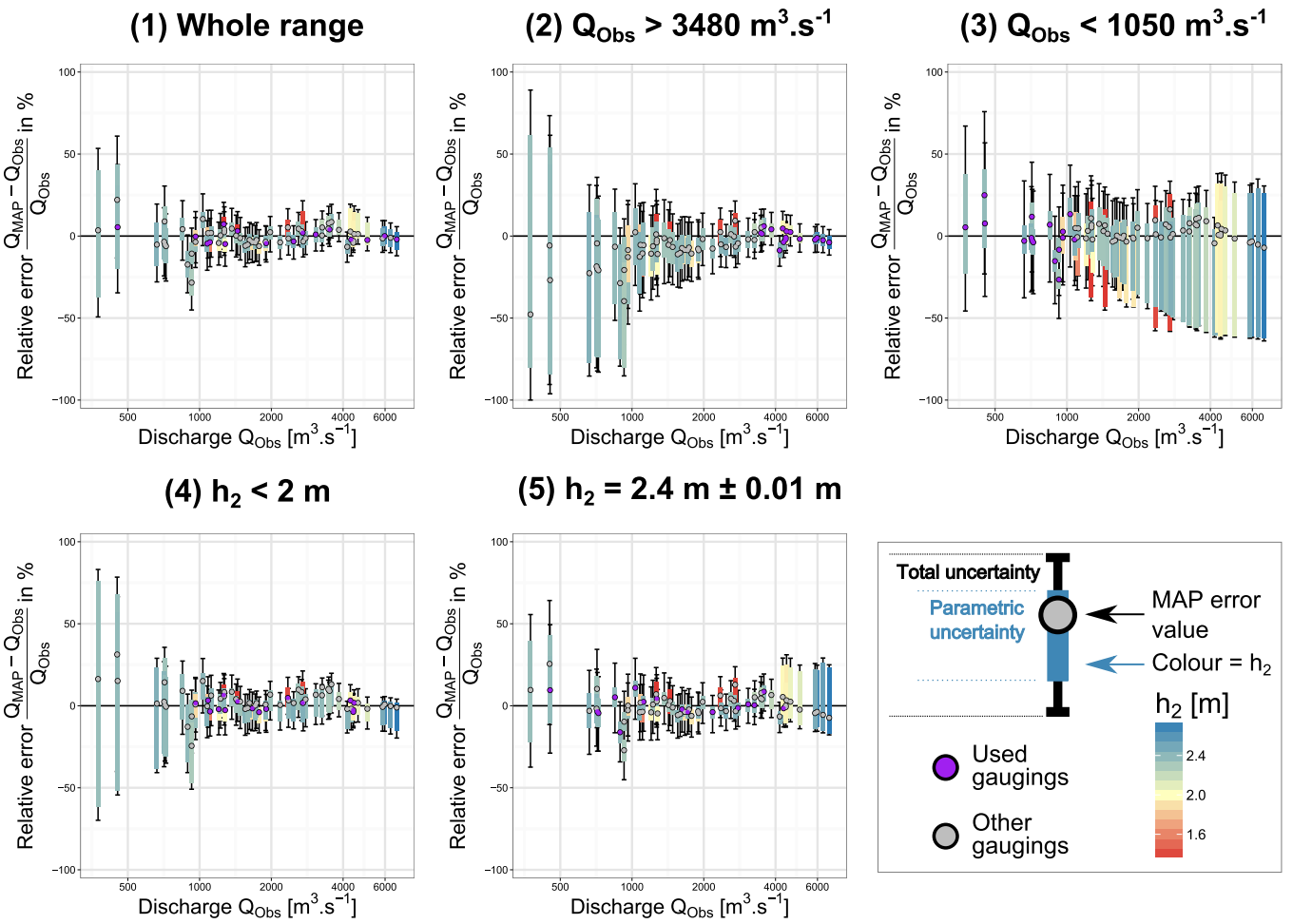


**Figure 9.** Sensitivity analysis of the stage-fall-discharge model to gauging dataset applied to the Rhône River at Valence: relative errors of estimated discharges compared to discharge observations $Q_{Obs}$ .$Q_{Obs}$ values are represented using a logarithm scale.

influenced by important variable backwater effect [*Callède et al.*, 2001] correlated with the yearly flood regime of the Amazon hydrosystem [*Callède et al.*, 2002].

The river bed is covered with large sand dunes. The dynamics and relative submergence of such bedforms induce flow resistance to vary with stage [e.g., *Karim*, 1995]. Flow resistance computed from the gaugings was indeed observed to increase with stage, toward an apparently asymptotic value (cf. Figure 10). The flow resistance coefficients can be computed using hydraulic radii from the gaugings bathymetry profiles by inverting the Manning-Strickler formula . As a first-order approach, possible hysteresis effects due to dune-flat bed transitions [*Shimizu et al.*, 2009] are ignored in this work.

As variable backwater effects are always present even during major floods, transition to an unaffected channel control is no longer needed. Equation (8) is modified for a single control rating curve as follows:

where the Strickler coefficient $K_S$ can be considered to be either constant () or to vary with stage. We propose the following empirical relation for modelling this stage-roughness relation:

where $\alpha$ is a coefficient, and are related to the high-flow asymptotic roughness. In the Bayesian analysis, the three parameters will be estimated as additional parameters of the SFD model.

Priors may be set up from the following considerations. Parameter $\alpha$ is expected to be positive since the Strickler coefficient (inverse to Manning's $n$) is expected to increase with increasing submergence of the bedforms. Assuming that cannot exceed the extreme value of , for a possible difference of between stage $h_1$ and $h_{channel}$, parameter $\alpha$ needs to be smaller than 1 (otherwise $K_S < 0$). Therefore, a uniform distribution is set up as prior

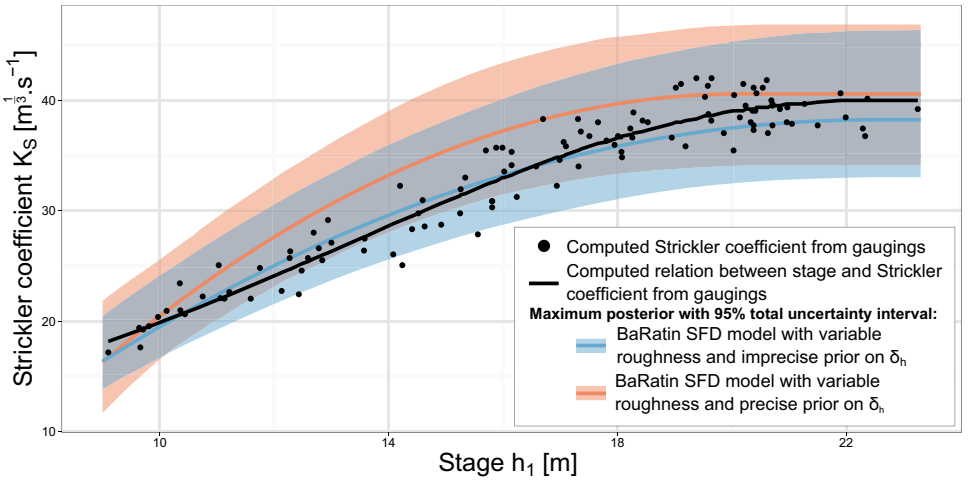


**Figure 10.** Strickler flow resistance coefficient of the Madeira River at Fazenda, as a function of stage at main gauge: data derived from gaugings, and empirical functions calibrated either manually or automatically with Bayesian SFD models.

on parameter $\alpha$. From the site configuration, the average roughness of the bankful channel is assessed to be . The stage is set up to .

The section between both gauges is a fairly straight reach with a mean width of which can vary () due to the presence of few small islands and a bend upstream of the auxiliary gauge. Cross-sectional shape is modeled as a wide rectangle, hence parameter $M$, the hydraulic exponent, is set to . The channel offset $h_0$ is set to from available cross-sectional profiles surveyed at the station. The official value of the datum difference $\delta_h$ is . This value comes from quite uncertain topography measurements, due to the long distances, the difficult maintenance of staff gauges in such mega-river sites, and departures between geographical reference systems and the gravity-based hydraulic heads. This value obviously leads to conflicts since it induces marked negative slope values at low flows whereas reverse flows were never gauged. Uncertainty of this parameter is accordingly imposed to , i.e., the imprecise prior is specified.

Prior distributions based on this information are detailed in Table 3. Three single-segment rating curve models are applied: constant slope channel control (SD model), SFD model with constant roughness, and SFD model with variable roughness.

The SFD model with variable roughness is applied considering either an imprecise or a precise prior on parameter $\delta_h$. Two comparisons are made: the impact of the roughness model and the impact of the parameter $\delta_h$ on the SFD model. The results are shown in Figure 11 and in Table 3. Figure 11 is the

**Table 3.** Bayesian Analysis of the Stage-Fall-Discharge (SFD) Rating Curves of the Madeira River at Fazenda Vista Alegre: Parameters, Prior Distributions and Maximum a Posteriori (MAP) Results With 2.5% and 97.5% Quantiles ($Q_{2.5}$ and $Q_{97.5}$)

| | | | Results: MAP[$Q_{2.5}$; $Q_{97.5}$] | | | |
|---|---|---|---|---|---|---|
| | | | | | SFD Model With $K_S(h_1)$ Variable | |
| BaRatin Parameters | Physical Parameters With Units | Prior Distributions | SD Model | SFD Model With Constant $K_S$ | Reasonable Prior $\delta_h \sim \mathcal{N}(-1.57, 1)$ | Precise But Inaccurate Prior $\delta_h \sim \mathcal{N}(-1.57, 0.01)$ |
| $\theta_1$ | $B$ (m) | $\mathcal{N}(1200, 100)$ | | | 1245 [1061; 1404] | 1296 [1096; 1436] |
| $\theta_1$ | $K_S B$ ($m^{\frac{1}{3}}.s^{-1}$) | $\mathcal{N}(42000, 3500)$ | | 46896 [42593; 52864] | | |
| $\theta_1$ | $K_S B\sqrt{S_0}$ ($m^{\frac{1}{3}}.s^{-1}$) | $\mathcal{N}(1328, 350)$ | 240 [197; 287] | | | |
| $\theta_2$ | $h_0$ (m) | $\mathcal{N}(-3, 0.5)$ | −1.58 [−2.62; −0.56] | 0.64 [−0.09, 2.40] | −2.90 [−3.72, −1.90] | −2.95 [−3.99; −2.11] |
| $\theta_3$ | $M = 5/3$ | $\mathcal{N}(1.6667, 0.025)$ | 1.697 [1.644, 1.746] | 1.780 [1.751, 1.828] | 1.687 [1.644, 1.725] | 1.674 [1.641; 1.725] |
| $\theta_4$ | $L$ (m) | $\mathcal{N}(92000, 500)$ | | 92021 [91017; 92951] | 92038 [91030; 92993] | 91749 [91038; 92906] |
| $\theta_5$ | $h_{\text{channel}}$ (m) | $\mathcal{N}(19, 2)$ | | | 22.46 [21.00; 23.99] | 20.13 [18.13; 21.43] |
| $\theta_6$ | $\alpha$ ($m^{-\frac{5}{3}}.s^{-1}$) | $\mathcal{U}(0, 1)$ | | | 0.121 [0.096; 0.161] | 0.196 [0.136; 0.318] |
| $\theta_7$ | $K_{\text{channel}}$ ($m^{\frac{1}{3}}.s^{-1}$) | $\mathcal{N}(35, 5)$ | | | 38.23 [33.04; 46.41] | 40.59 [34.09; 46.88] |
| $\theta_8$ | $\delta_h$ (m) | $\mathcal{N}(-1.57, 1)$ | | −1.90 [−2.05; −1.83] | −1.98 [−2.03; −1.92] | −1.59 [−1.62, −1.58] |
| $\gamma_1$ | $m^3.s^{-1}$ | $\mathcal{U}(0, 10^6)$ | 8596 [3189; 9324] | 2060 [186; 2537] | 126 [13; 598] | 2472 [2063; 2874] |
| $\gamma_2$ | | $\mathcal{U}(0, 10^6)$ | 0.00024 [0.0011; 0.19] | 0.0022 [0.00047; 0.052] | 0.041 [0.024; 0.054] | 0.00015 [0.00011; 0.013] |

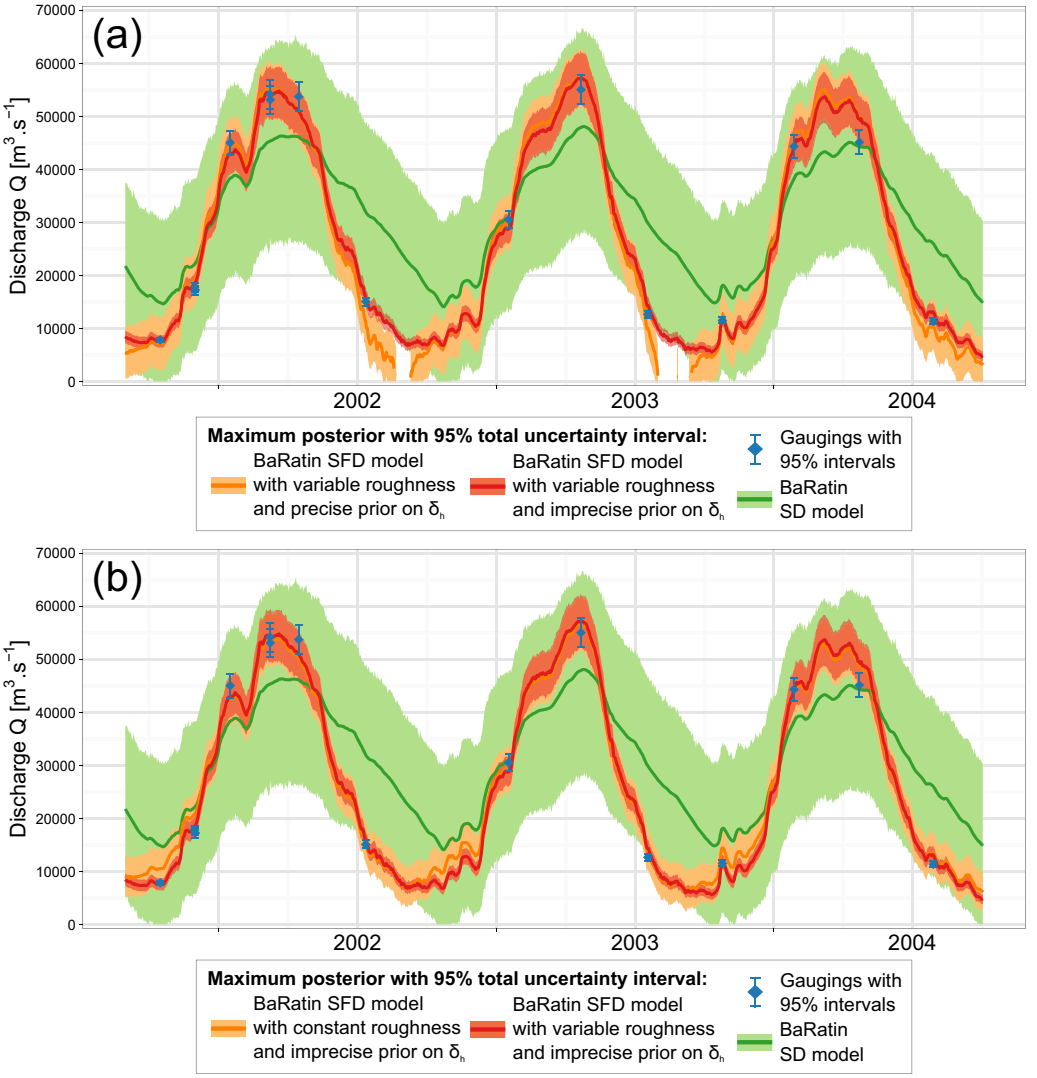


**Figure 11.** The Madeira River at Fazenda over the 2001–2004 period: gaugings, MAP computed flow records and their 95% total uncertainties envelopes. (a) the SFD model with variable roughness is used for a comparison between two prior distributions on the datum difference $\delta_h$: imprecise prior (± 127% uncertainty) versus precise prior (± 1.27% uncertainty). (b) comparison of the variable and constant roughness options, both for a imprecise prior on $\delta_h$. In both graphs, the results from the standard stage-discharge (SD) model are also plotted.

propagation of the estimated rating curves from those three models over the 2001–2004 period (3 hydrological years). Figure 11a corresponds to the comparison between the two prior options on the $\delta_h$ parameter for the SFD model with variable roughness, Figure 11b is the comparison between the constant roughness and the variable roughness options in the SFD model. All the models illustrate the yearly flood cycles: 3 floods over this period with, for each flood, approximatively 5 months of rising limb and 7 months of falling limb.

The stage-discharge (SD) model is not appropriate for capturing the variable backwater effects. The maximum posterior (MAP) curve markedly overestimates discharges (up to more than 100%) at low flows and underestimates them (down to −11%) at high flows (cf. Figure 11). Related uncertainties are very large (up to more than  at low flows and never less than ).

### 5.2. Variable Roughness and Influence of Datum Difference $\delta_h$

Both SFD models with or without variable roughness yield good results at high flows: MAP curves agree well with gaugings and uncertainties fluctuate around  of the discharge. At low flows the constant roughness option is unable to keep up the better results of the variable roughness option (Figure 11b). For

discharges lower than , uncertainties are larger (between and ) than for the variable roughness option (less than ).

The constant roughness option implies a calibration of the roughness parameter on the whole range of flow. This calibration leads to an overestimation of the roughness value: the model adjusts parameters $h_0$ and $M$ to compensate for this high value. This leads to unrealistic values for the two parameters. The exponent value (1.78, in Table 3), though realistic, does not match with the hydraulic assumptions of a wide rectangular cross-section (prior value ). All these results clearly show that accounting for the measured variable slope may not be enough to accurately estimate low flows, when modelling a variable roughness is also required.

Different priors on $\delta_h$ appear not to affect high flow estimates (Figure 11a): MAP values and uncertainty envelopes are the same whether or not the prior on $\delta_h$ is imprecise. Indeed, for high flows, the parameter $\delta_h$ has less influence on the computation of the variable slope. The stage-roughness (Strickler coefficient) relation is moderately affected by the prior information on $\delta_h$ (cf. Figure 10). The widths of the uncertainty envelopes are the same but the MAP curves for precise but inaccurate prior on $\delta_h$ is further away from the manually computed Strickler coefficient curve. A too precise but inaccurate prior on $\delta_h$ also involves higher uncertainties at low flows. Below , uncertainties on discharges fluctuate between and more than instead of less than using a imprecise prior. The slope is sometimes estimated to be negative over periods where reverse flows were never gauged nor observed. Then the result is discarded and no discharge is computed (cf. blank spaces in Figure 11a in the beginning of years 2002 and 2003 for the BaRatin SFD model with variable roughness and precise prior on $\sigma_h$). Therefore, in such a case the datum difference $\delta_h$ is preferred to be estimated from gaugings, as a free parameter of the SFD model. The prior uncertainty on this parameter

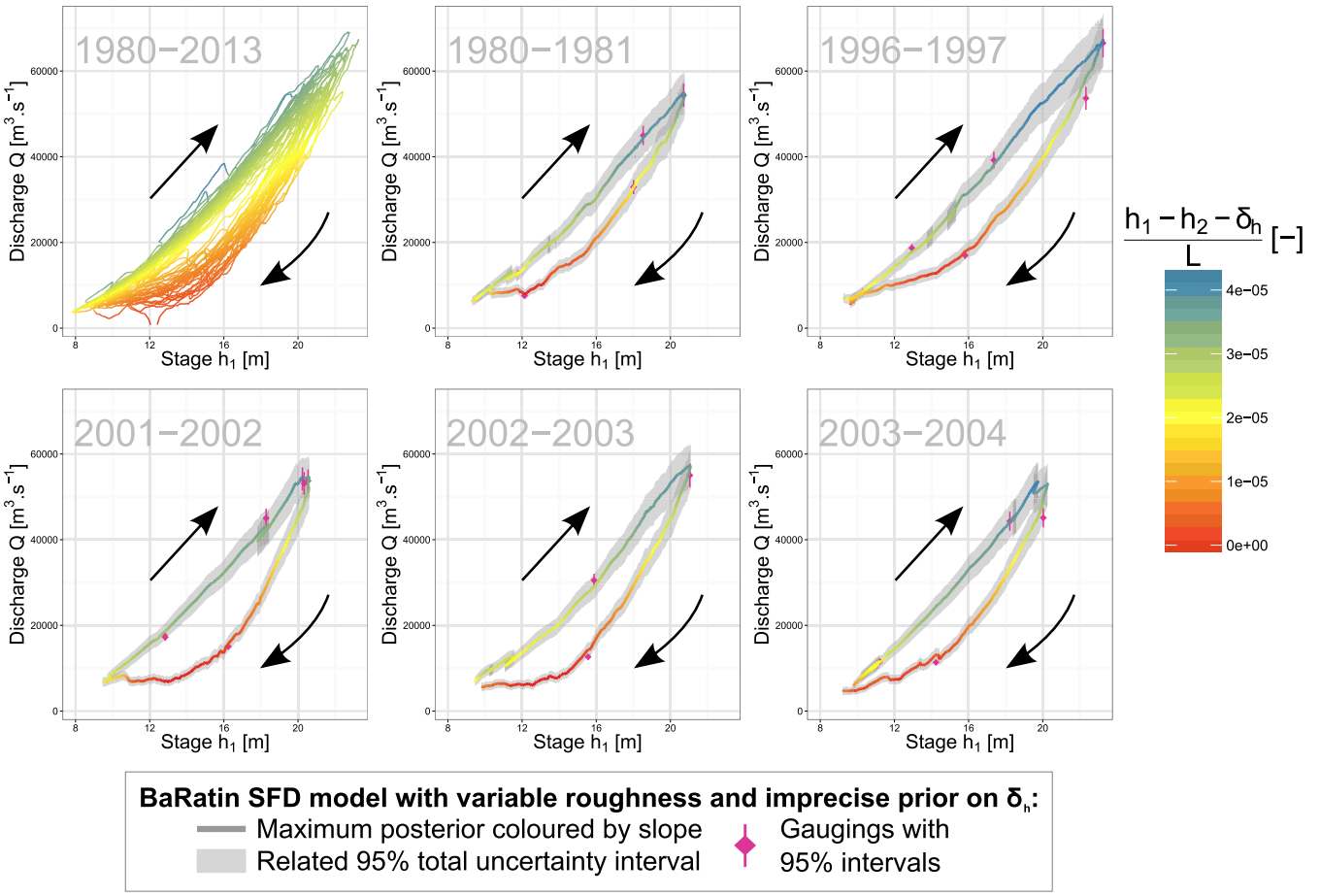


**Figure 12.** The Madeira River at Fazenda: stage-discharge representation of the results from the SFD model with variable roughness and imprecise prior on datum difference $\delta_h$. Maximum a posteriori (MAP) rating curves for the 1980–2013 period and five contrasted hydrological years are coloured according to the computed energy slope $(h_1 - h_2 - \delta_h)/L$.

has to be set up according to each situation but can be kept reasonably wide since this parameter has little interaction with the other ones.

The BaRatin SFD model with variable roughness and imprecise prior on $\delta_h$ parameter yields good discharge estimations. Despite some very uncertain gaugings, MAP error values are always under 10% for the other gaugings (under 20% for all). Associated total uncertainty envelopes are also acceptable (less than  for low flows and less than  for discharges ). This case illustrates the limitations of the stage-fall-discharge approach: when flow resistance also varies as a function of flow depth, this has to be captured in the rating curve model in addition to the variable slope due to backwater effects. It also illustrates the importance of reflecting the real uncertainties of the prior information on the datum difference, $\delta_h$, to accurately model low flow discharges.

### 5.3. A Flood-Specific Rating Curve

For a better understanding of the BaRatin SFD model with variable roughness according to the yearly flood cycles, stage-discharge relations are represented in Figure 12. MAP rating curves and their total uncertainty envelopes over the 1980–2013 period are represented as well as for 5 contrasted hydrological years.

The rating curve of such phenomenon plots as a loop  relation (cf. Figure 12). The size and opening of the SFD rating curve of the Fazenda station depend on the magnitude of the Madeira flood and of the Amazon flood, respectively. The loops have the same direction as rating curves affected by hysteresis due to transient flows but differ by their characteristic bow-shapes: during the rising limb, the  relation is more linear than during the falling limb, opposite to the usual shape of the hysteretic rating curves. The station is less influenced by the Amazon flows during the rising limb: the downstream and upstream stages increase in similar proportions. Conversely, during the falling limb the influence of the Amazon main stem increases. The energy slope decreases as the upstream stage $h_1$ decreases but the downstream stage decreases slowly, due to the slower dynamics of the Amazon flood. Energy slope values are then smaller than during the rising limb.

## 6. Conclusions and Perspectives

To avoid some assumptions made in the model proposed by *Petersen-Øverleir and Reitan* [2009] for the Bayesian analysis of stage-fall-discharge rating curves, we introduced an alternative model accounting for transition between a backwater-affected control and a backwater-unaffected control. The main differences lie in the definition of distinct parameters for both controls and in solving transition between controls using continuity conditions only. The new model also acknowledges the uncertain nature of the difference in reference levels of the main and auxiliary gauges.

The robustness of this new model was investigated through sensitivity analyses to the prior information and to the gaugings data set. When the stage-fall-discharge domain is well documented with gaugings, the performance of the new model appears to be acceptable for hydrometric applications. In particular, transition to backwater-unaffected flow was correctly simulated in the Rhône River at Valence station, discharge estimates are in good agreement with gaugings, and uncertainty bounds are usually acceptable. The example of a section control combined with a variable slope channel control (Guthusbekken) yielded acceptable though less convincing results, likely due to limitations in both hydraulic knowledge and gaugings available at that site.

A challenging channel-controlled case, the Madeira at Fazenda Vista Alegre, eventually showed the limitations of the stage-fall-discharge approach: in that large sand-bed river with large dune systems, flow resistance also varies as a function of flow depth, and this has to be captured in the rating curve model, in addition to variable slope due to backwater from the Amazon main stem. This difficult case also illustrates the interest of estimating the difference in staff gauge reference levels, when this parameter bears nonnegligible uncertainties.

With such improvements brought to the Bayesian approach initiated by *Petersen-Øverleir and Reitan* [2009], the method now appears as a mature and credible solution to the issue of stage-fall-discharge rating curves, and as a substitution for the graphical and empirical techniques still proposed in hydrometry guidance and standards [e.g., *ISO 9123*, 2001]. It has been operationally deployed by the Compagnie Nationale du Rhône

(CNR) for developing SFD rating curves at their twin-gauge stations. The method provides rating curve results in both functional and table formats; uncertainty results come as probabilistic distributions from which any statistics can be derived. The uncertainty analysis is compliant with the concepts of the Guide for the expression of the Uncertainty in Measurement (GUM) [e.g., *JCGM 100*, 2008] and could embed the propagation of stage record uncertainties.

## References


Callède, J., P. Kosuth, and E. De Oliveira (2001), Etablissement de la relation hauteur-débit de l'Amazone à Óbidos: Méthode de la dénivelée normale à "géométrie variable," *Hydrol. Sci. J.*, *46*(3), 451–463, doi:10.1080/02626660109492838.

Callède, J., J.-L. Guyot, J. Ronchail, M. Molinier, and E. De Oliveira (2002), L'Amazone à Óbidos (Brésil): Etude statistique des débits et bilan hydrologique, *Hydrol. Sci. J.*, *47*(2), 321–333, doi:10.1080/02626660209492933.

Coxon, G., J. Freer, I. K. Westerberg, T. Wagener, R. Woods, and P. J. Smith (2015), A novel framework for discharge uncertainty quantification applied to 500 UK gauging stations, *Water Resour. Res.*, *51*, 5531–5546 doi:10.1002/2014WR016532.

Despax, A., C. Perret, R. Garo¸n, A. Hauet, A. Belleville, J. Le Coz, and A.-C. Favre (2016), Considering sampling strategy and cross-section complexity for estimating the uncertainty of discharge measurements using the velocity-area method, *J. Hydrol.*, *533*, 128–140, doi:10.1016/j.jhydrol.2015.11.048.

Fenton, J. D., and R. J. Keller (2001), The calculation of streamflow from measurements of stage, *Tech. Rep. 01/6*, Coop. Res. Cent. for Catchment Hydrol., University of Canberra ACT 2601, Canberra, Australia. [Available at http://www.ewater.org.au/archive/crcch/.]

Hall, M. R., W. E. Hall and C. H. Pierce (1915), A method of determining the daily discharge of rivers of variable slope, *U. S. Geol. Surv. Water Supply Pap.*, *345 E-*, 53–61.

Hidayat, H., B. Vermeulen, M. G. Sassi, P. J. J. F. Torfs, and A. J. F. Hoitink (2011), Discharge estimation in a backwater affected meandering river, *Hydrol. Earth Syst. Sci.*, *15*(8), 2717–2728, doi:10.5194/hess-15-2717-2011.

Hoitink, A. J. F., F. A. Buschman, and B. Vermeulen (2009), Continuous measurements of discharge from a horizontal acoustic Doppler current profiler in a tidal river, *Water Resour. Res.*, *45*, doi:10.1029/2009WR007791.

ISO 9123 (2001), *Measurement of Liquid Flow In Open Channels—Stage-Fall-Discharge Relationships*, 14 p., Int. Organ. for Stand., Geneva, Switzerland.

ISO 1100-2 (2010), *Hydrometry—Measurement of Liquid Flow in Open Channels Part 2: Determination of the Stage-Discharge Relationship*, 28 pp., Int. Organ. for Stand., Geneva, Switzerland.

ISO/TS 25377 (2007), *Hydrometric Uncertainty Guidance (HUG)*, 51 pp., Int. Organ. for Stand., Geneva, Switzerland.

JCGM 100 (2008), *Evaluation of Measurement Data—Guide to the Expression of Uncertainty in Measurement (GUM)*, 120 pp., JCGM Member Organ, BIPM, Sèvres, France.

Jones B. E. (1916), A method of correcting river discharge for a changing stage, *U. S. Geol. Surv. Water Supply Pap.*, *375 E*, 117–130.

Juston, J., P.-E. Jansson, and D. Gustafsson (2014), Rating curve uncertainty and change detection in discharge time series: Case study with 44-year historic data from the Nyangores River, Kenya, *Hydrol. Processes*, *28*, 2509–2523, doi:10.1002/hyp.9786.

Karim, F. (1995), Bed configuration and hydraulic resistance in alluvial-channel flows. *J. Hydraul. Eng.*, *121*(1), 15–25, doi:10.1061/(ASCE)0733-9429(1995)121:1(15).

Latrubesse, E. M. (2008), Patterns of anabranching channels: The ultimate end-member adjustment of mega rivers, *Geomorphology*, *101*(1), 130–145, doi:10.1016/j.geomorph.2008.05.035.

Le Coz, J., G. Pierrefeu, and A. Paquier (2008), Evaluation of river discharges monitored by a fixed side-looking Doppler profiler, *Water Resour. Res.*, *44*, W00D09, doi:10.1029/2008WR006967.

Le Coz, J., B. Renard, L. Bonnifait, F. Branger and R. Le Boursicaud (2014), Combining hydraulic knowledge and uncertain gaugings in the estimation of hydrometric rating curves: A Bayesian approach, *J. Hydrol.*, *509*, 573–587, doi:10.1016/j.jhydrol.2013.11.016.

Le Coz, J., B. Blanquart, K. Pobanz, G. Dramais, G. Pierrefeu, A. Hauet and A. Despax (2016), Estimating the uncertainty of streamgauging techniques using in situ collaborative interlaboratory experiments, *J. Hydraul. Eng.*, *142*(7), 04016011, doi:10.1061/(ASCE)HY.1943-7900.0001109.

Levesque, V. A. and K. A. Oberg (2012), Computing discharge using the index velocity method, *U.S. Geol. Surv. Tech. Methods*, *3–A23*, 148 pp. [Available at http://pubs.usgs.gov/tm/3a23/.]

McMillan, H. K., and I. K. Westerberg (2015), Rating curve estimation under epistemic uncertainty, *Hydrol. Processes*, *29*(7), 1873–1882, doi:10.1002/hyp.10419.

McMillan, H. K., J. Freer, F. Pappenberger, T. Krueger, and M. Clark (2010), Impacts of uncertain river flow data on rainfall-runoff model calibration and discharge predictions, *Hydrol. Processes*, *24*(10), 1270–1284, doi:10.1002/hyp.7587.

Morlot, T., C. Perret, A. C. Favre, and J. Jalbert (2014), Dynamic rating curve assessment for hydrometric stations and computation of the associated uncertainties: Quality and station management indicators, *J. Hydrol.*, *517*, 173–186, doi:10.1016/j.jhydrol.2014.05.007.

Moyeed, R. A., and R. T. Clarke (2005), The use of Bayesian methods for fitting rating curves, with case studies, *Adv. Water Resour.*, *28*(8), 807–818, doi:10.1016/j.advwatres.2005.02.005.

Nihei, Y., and A. Kimizu (2008), A new monitoring system for river discharge with horizontal acoustic Doppler current profiler measurements and river flow simulation, *Water Resour. Res.*, *44*, W00D20, doi:10.1029/2008WR006970.

Petersen-Øverleir, A., and T. Reitan (2009), Bayesian analysis of stage-fall-discharge models for gauging stations affected by variable backwater, *Hydrol. Processes*, *23*(21), 3057–3074, doi:10.1002/hyp.7417.

Rantz, S. E. (1982), Measurement and computation of streamflow. Volume 2: Computation of discharge, *U.S. Geol. Surv. Water Supply Pap.*, *2175*, 631 pp.

Reitan, T., and A. Petersen-Øverleir (2008), Bayesian power-law regression with a location parameter, with applications for construction of discharge rating curves, *Stochastic Environ. Res. Risk Assess.*, *22*(3), 351–365, doi:10.1007/s00477-007-0119-0.

Réméniéras, G. (1949), *Annuaire hydrologique de la France, année 1949: L'Hydraulique des stations limnimétriques pour la mesure du débit des cours d'eau*, Soc. Hydrotechnique de France, SHF, Paris, France.

Renard, B., V. Garreta, and M. Lang (2006), An application of Bayesian analysis and Markov chain Monte Carlo methods to the estimation of a regional trend in annual maxima, *Water Resour. Res.*, *42*, W12422, doi:10.1029/2005WR004591.

Schmidt, A.R. (2002), Analysis of stage-discharge relations for open-channel flows and their associated uncertainties, PhD thesis, Univ. of Illinois, Urbana-Champaign.



**Acknowledgments**

The PhD fellowship of V. Mansanarez is funded by Irstea and the Compagnie nationale du Rhône (CNR), with the support of the French national hydrological services (SCHAPI). The FloodScale project is funded by the French National Research Agency (ANR) under contract ANR 2011 BS56 027, which contributes to the HyMeX program. We also wish to acknowledge the research funding provided by the Région Rhône-Alpes (Explora'doc). The use of the data of the Madeira River at Fazenda was possible thanks to the Brazilian National Water Agency (ANA), the Brazil Geological Survey (CPRM) and the HyBAM observation service. These data are available online (http://www.ore-hybam.org/index.php/eng) from the HyBAM observation service following registration. Data for the Guthusbekken station were made available online by Trond Reitan (http://folk.uio.no/trondr/hydrasub/ratingcurve.html). Data for the Valence station were provided by CNR (special thanks to Karine Pobanz and Raphaël Le Boursicaud). These data are available from the authors upon request (g.pierrefeu@cnr.tm.fr). BaRatin uses the DMSL Fortran library developed by Dmitri Kavetski (University of Adelaide, Australia).

Shimizu, Y., S. Giri, S. Yamaguchi, and J. Nelson (2009), Numerical simulation of dune-flat bed transition and stage-discharge relationship with hysteresis effect, *Water Resources Research*, *45* W04429, doi:10.1029/2008WR006830.

Shrestha, R. R., A. Bárdossy, and F. Nestmann (2007), Analysis and propagation of uncertainties due to the stagedischarge relationship: A fuzzy set approach, *Water Resour. Res.*, *45* W04429, doi:10.1029/2008WR006830.

Sikorska, A. E., A. Scheidegger, K. Banasik, and J. Rieckermann (2013), Considering rating curve uncertainty in water level predictions, *Hydrol. Earth Syst. Sci.*, *17*(11), 2955–2986, doi:10.5194/hess-17-4415-2013.

Westerberg, I. K., J.-L. Guerrero, J. Seibert, K. J. Beven, and S. Halldin (2011), Stage-discharge uncertainty derived with a non-stationary rating curve in the Choluteca River, Honduras, *Hydrol. Processes*, *25*, 603–613, doi:10.1002/hyp.7848.

World Meteorological Organization (2010), Manual on stream gauging. Volume II—Computation of discharge, *WMO 1044*, 195 pp.